ISSN 1069-3513, Izvestiya, Physics of the Solid Earth, 2015, Vol. 51, No. 2, pp. 268–277. © Pleiades Publishing, Ltd., 2015.
Original Russian Text © A.K. Nekrasova, V.G. Kossobokov, I.A. Parvez, 2015, published in Fizika Zemli, 2015, No. 2, pp. 116–125.

Seismic Hazard and Seismic Risk Assessment Based on the Unified Scaling Law for Earthquakes: Himalayas and Adjacent Regions

A. K. Nekrasova[a], V. G. Kossobokov[a, b], and I. A. Parvez[c]

[a] *Institute of Earthquake Prediction Theory and Mathematical Geophysics, Russian Academy of Sciences, ul. Profsoyuznaya 84/32, Moscow, 117997 Russia*

e-mail: nastia@mitp.ru, volodya@mitp.ru

[b] *Institut de Physique du Globe de Paris, Paris, France*

e-mail: volodya@ipgp.fr

[c] *Centre for Mathematical Modelling and Computer Simulation, Council of Scientific and Industrial Research, Bangalore, India*

e-mail: parvez@cmmacs.ernet.in

Received June 13, 2013; in final form, September 30, 2014

Abstract—For the Himalayas and neighboring regions, the maps of seismic hazard and seismic risk are constructed with the use of the estimates for the parameters of the unified scaling law for earthquakes (USLE), in which the Gutenberg–Richter law for magnitude distribution of seismic events within a given area is applied in the modified version with allowance for linear dimensions of the area, namely, $\log N(M, L) = A + B(5 - M) + C\log L$, where $N(M, L)$ is the expected annual number of the earthquakes with magnitude M in the area with linear dimension L. The spatial variations in the parameters A, B, and C for the Himalayas and adjacent regions are studied on two time intervals from 1965 to 2011 and from 1980 to 2011. The difference in A, B, and C between these two time intervals indicates that seismic activity experiences significant variations on a scale of a few decades. With a global consideration of the seismic belts of the Earth overall, the estimates of coefficient A, which determines the logarithm of the annual average frequency of the earthquakes with a magnitude of 5.0 and higher in the zone with a linear dimension of 1 degree of the Earth's meridian, differ by a factor of 30 and more and mainly fall in the interval from −1.1 to 0.5. The values of coefficient B, which describes the balance between the number of earthquakes with different magnitudes, gravitate to 0.9 and range from less than 0.6 to 1.1 and higher. The values of coefficient C, which estimates the fractal dimension of the local distribution of epicenters, vary from 0.5 to 1.4 and higher. In the Himalayas and neighboring regions, the USLE coefficients mainly fall in the intervals of −1.1 to 0.3 for A, 0.8 to 1.3 for B, and 1.0 to 1.4 for C. The calculations of the local value of the expected peak ground acceleration (PGA) from the maximal expected magnitude provided the necessary basis for mapping the seismic hazards in the studied region. When doing this, we used the local estimates of the magnitudes which, according to USLE, corresponded to the probability of exceedance 1% and 10% during 50 years or, if the reliable estimate is absent, the maximal magnitudes reported during the instrumental period. As a result, the seismic hazard maps for the Himalayas and the adjacent regions in terms of standard seismic zoning were constructed. Based on these calculations, in order to exemplify the method, we present a series of seismic risk maps taking into account the population density prone to seismic hazard and the dependence of the risk on the vulnerability as a function of population density.

DOI: 10.1134/S1069351315010103

INTRODUCTION

Earthquakes are among the most hazardous disasters. The sudden character of a seismic event can instantly lead to considerable destruction and human deaths. Earthquakes occur in the form of a propagating rupture that releases the tectonic stresses accumulated in the system of lithospheric blocks and the faults between them. The territory of the Himalayas and adjacent regions was hit by a few devastating earthquakes with magnitudes 8 and higher, which caused heavy losses and considerable economic damage in the past. One of the ways to mitigate the destruction effect from earthquakes is to analyze seismic hazards and implement the corresponding preventive safety measures. The errors in seismic hazard assessment may and do cause unpredicted fatalities and economic losses (Wyss et al., 2012). Clearly, the economic losses include both the unbudgeted expenditures for infrastructure repairs in the earthquake-damaged areas where seismic hazard was underestimated and those for excessive safety measures in the areas where seismic hazard was overestimated.

Of course, an earthquake is a very complex natural phenomenon, but its complexity still possesses a certain order. The distribution of seismic events is likely to be self-similar (Mandelbrot, 1982; Keilis-Borok, 1990; Turcotte, 1997; 1999) and enables scaling in accordance with the generalized Gutenberg–Richter recurrence law, which takes into account the fractal character of spatial distribution of the earthquakes' epicenters (Kossobokov and Mazhkenov, 1988). Clearly, in the case of the uniform distribution of the epicenters on the surface, their number will be proportional to the size of a given area (for example, a circle or square), whereas if the epicenters are clustered along a line or within a narrow band (for example, in the linear fault zone), the number of the events will be proportional to the linear dimension of the area (for example, a radius of the circle or a side of the square, respectively). There are also examples of spatial distributions that correspond to a fractional dimension of the fractal support of the epicenters, which cannot be excluded a priori and are verified by the independent data (Okubo and Aki, 1987; Sadovskii et al., 1982; 1984). It is also worth noting that seismic activity is far from being temporally uniform.

Thus, the question of the spatial and time scales unavoidably emerges in the problems of seismic hazard and seismic risk assessment and, in particular, in the studies of the series of the earthquakes for predicting large seismic events, where it is required to transfer the estimates, rules, and criteria from one spatiotemporal domain to another. With sufficient data on the earthquakes, the estimates of the coefficients in the unified scaling law for earthquakes (USLE) can provide a reliable solution to this problem (Kossobokov and Nekrasova, 2003, 2004). The USLE generalizes the Gutenberg–Richter law of frequency–magnitude distribution for seismic events within a given area in the following modified form, which takes into account the fractal nature of the support of the epicenters:

$$\log N(M, L) = A + B(5 - M) + C\log L, \qquad (1)$$

where $N(M, L)$ is the expected annual number of earthquakes with magnitude M in an area with linear dimension L; $\log X$ is the common logarithm of X.

Bak et al. (2002) and Christensen et al. (2002) suggested the version of USLE in terms of inter-event time. Obviously, the time between the earthquakes is dual, i.e., in inverse proportion, to the number of the earthquakes during a unit time interval in formula (1).

Despite the difficulties mentioned above, the problem of seismic hazard assessment for the territory of the Himalayas and adjacent regions was addressed in many studies (e.g., Auden, 1959; Gaur and Choudan, 1968; Kaila and Rao, 1979; Khattri et al., 1984; Parvez and Ram, 1997; 1999; Parvez et al., 2003; Parvez, 2007; Bhatia et al., 1999; Lyubushin and Parvez, 2010). In the present paper, we assume the hypothesis that seismic process is self-similar, at least locally, and calculate the coefficients of A, B, and C by the SCE (Scaling Coefficients Estimation) algorithm for estimating the scaling coefficients based on the data of the Global Hypocenters Database System (Nekrasova and Kossbokov, 2006; Nekrasova, 2008). The results are presented in the maps of USLE coefficients for different space and time scales; their probable correlation to the observed deformations of the subcontinent and corresponding tectonic structures is discussed. The estimates of the USLE coefficients are also used for calculating the seismic hazard in the region. Besides, we present the examples of different estimates of seismic risk for the Himalayas and the adjacent territories based on the obtained seismic hazard maps and the data on the population in the studied area.

METHOD

The results of global and regional analyses (Keilis-Borok et al., 1989; Kossobokov and Mazhkenov, 1994; Kossobokov and Nekrasova, 2004; Nekrasova et al., 2011) show that in the seismically active regions, the average annual number $N(M, L)$ of earthquakes with magnitude M in the structures of the embedded areas $L \times L$ with linear dimension L, within a wide range of magnitudes $M \in (M_-, M_+)$ and linear dimensions $L \in (L_-, L_+)$ agrees with the following formula of self-similarity:

$$N(M, L) = 10^A \times 10^{B\times(5-M)} \times L^C, \qquad (1')$$

where A, B, and C are the constants locally characterizing the logarithms of the annual average frequency of earthquakes with magnitude 5.0 and higher in the area with a linear dimension of 1 degree of the Earth's meridian, the balance between the number of earthquakes with different magnitudes, and the fractal dimension of the support of the earthquake epicenters, respectively.

The values of A, B, and C are calculated by the SCE algorithm for estimating the USLE scaling coefficients (Nekrasova, 2008).

The long-term estimates of the USLE coefficients can be used for characterizing the seismic hazard in terms of the expected maximal magnitude:

(a) For cells with centers on the regular mesh $l \times l$ and sizes $L_0 \times L_0$, where $L_0 \in (L_-, L_+)$ is a selected constant determined by analyzing the completeness of the data, coefficients A, B, and C are calculated.

(b) By formula (1), the expected number of the events during a given time interval of T years, $N_T(M, L_0) = T \times N(M, L_0)$, is determined for the considered cells and magnitudes M (with a step of Δm) in the interval from M_- to M_+.

(c) Based on a given threshold of probability p, the maximal magnitude M, for which the expected number of the earthquakes in the cell, $N_T(M, L_0)$, exceeds 1.

It can be expected on average that with confidence $1-p$, the magnitude determined this way for every cell

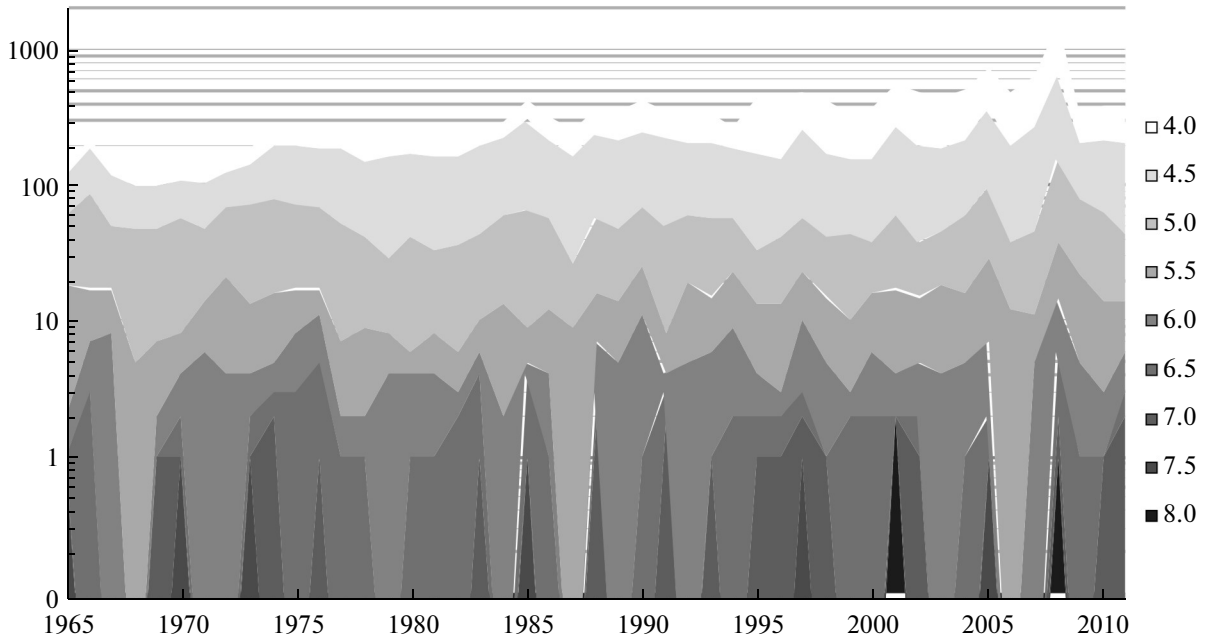

Fig. 1. The annual number of earthquakes exceeding the threshold magnitude in the Himalayas and adjacent areas.

will correspond to the maximal magnitude expected during the time interval T.

DATA

Seismic Data

The studied territory is located between 5° and 40° N, 60° and 105° E. We analyze the seismic events with magnitudes starting from 5 and hypocenters at depths less than 100 km from the USGS/NEIC Global Hypocenters Database System, 1965–2011. The 100-km depth limit is selected in accordance with the first local minimum in the distribution density of the hypocenters' depths within the studied territory. In the analysis, we use the maximal magnitude of those presented in the NEIC catalog (average *mb*, average M_S, and two authoritative magnitudes (among which, *MwHRV* and *MwGS* have become recently predominant). During the last 47 years, about 5000 earthquakes occurred in the studied territory. Figure 1 shows the fluctuations in the annual number of these events from 1965 to 2011. The annual average number of the earthquakes was quite stable (about 100–200 events per annum) until the mega-earthquake of December 26, 2004, whose epicenter, in contrast to the considerable part of its aftershocks, was located outside the studied territory. The spatial distribution of the empirical density of seismic events (the total sum of general density in the considered domain is 1) for the geographic grid with cells 0.5° × 0.5° in size is presented in Fig. 2. The color of the cells corresponds to the value of the empirical density function (on the logarithmic scale). The cells shown in Fig. 2 are the base on the hierarchical system of the areas with linear dimensions of 0.5°, 1°, 2°, 4°, and 8°, which are used in the calculation of the USLE coefficients. The reliable estimates of the USLE coefficients are obtained in 1143 of the 1150 cells shown in Fig. 2.

Data on Population Density

The estimates for the population density (per km^2) are available from the model of the Gridded Population of the World (2005), which was obtained as a result of processing the data collected by the Center for International Earth Science Information Network (CIESIN), Columbia University, United States, and by the International Center for Tropical Agriculture (Centro Internacional de Agricultura, CIAT), Colombia. The model provides the worldwide estimates of the population in 2005, 2010, and 2015 on the scales and with the degree of detail necessary for illustrating the spatial relationships between human populations and environmental protection all over the world. The model simulations are based on the censuses and spatially particularized data on the population density, which are compatible with the social, economical, and Earth Science data. In the present work, the model simulation of population for 2010 (GWPv3 version software) with a spatial resolution of 0.25° × 0.25° over the studied area within 5° to 40° N and 60° to 105° E is used. Figure 3 shows the spatial distribution of the population P per km^2 used in our analysis.

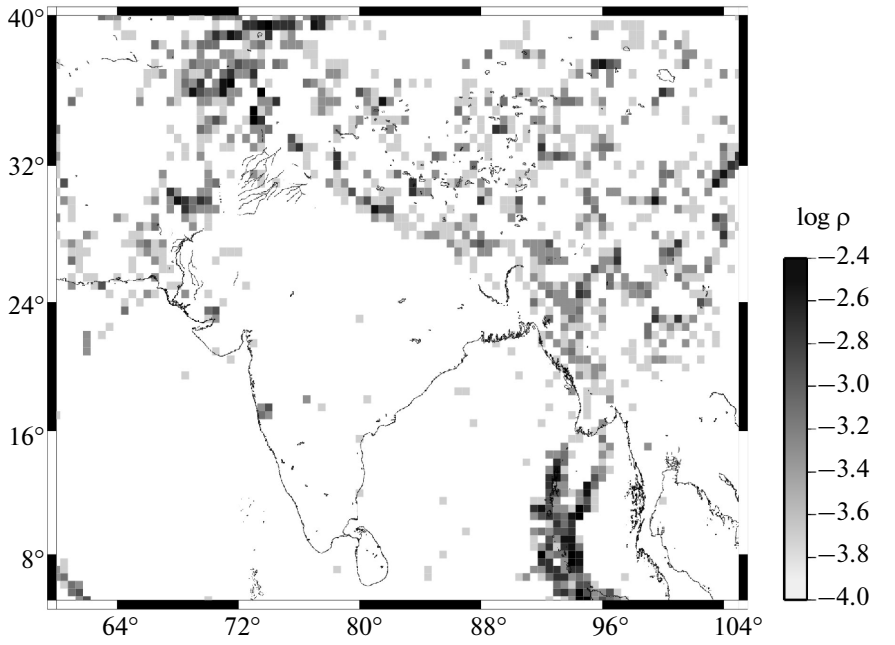

Fig. 2. Spatial distribution of the empirical probability density for the earthquakes with magnitude 5.0 and higher (ρ) in the studied territory, based on the USGS/NEIC Global Hypocenters Database System for the period of 1965 to 2011.

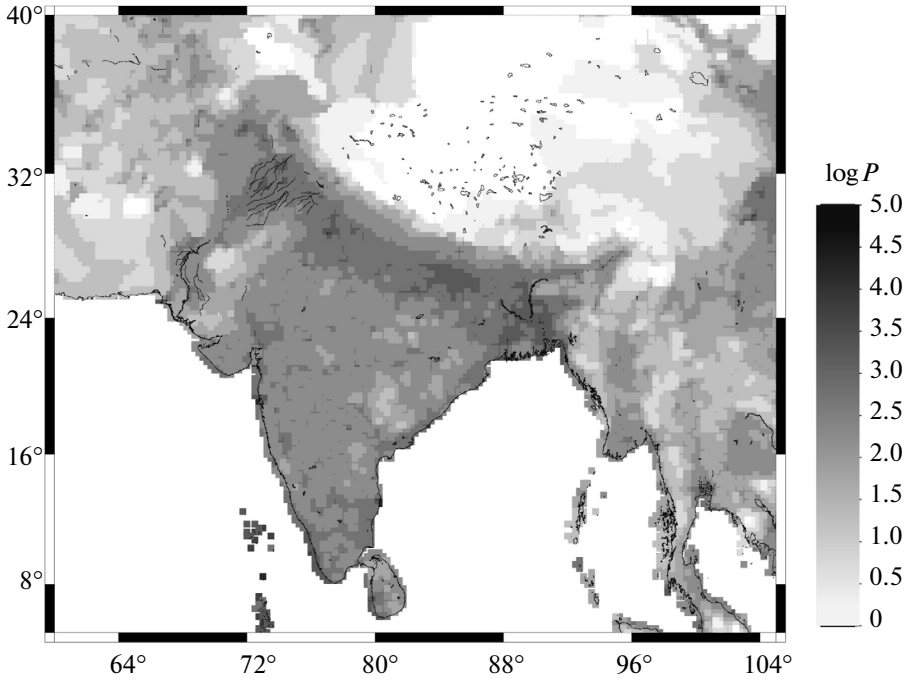

Fig. 3. Population density map with a resolution of 1 km^2 (based on GPWv3 estimate for 2010).

RESULTS

Seismic Hazard Assessment

Figure 4 shows the spatial distributions of the estimates for each of three USLE coefficients (*A*, which describes the logarithm of seismic activity; *B*, reflecting the balance between the neighboring bins of the magnitude range; and *C*, which corresponds to the estimate of the fractal dimension of the spatial distribution of the seismic sources). For interpretation purposes in this analysis, e.g., in Fig. 4, coefficient *A* is calibrated to fit the recurrence of strong earthquakes

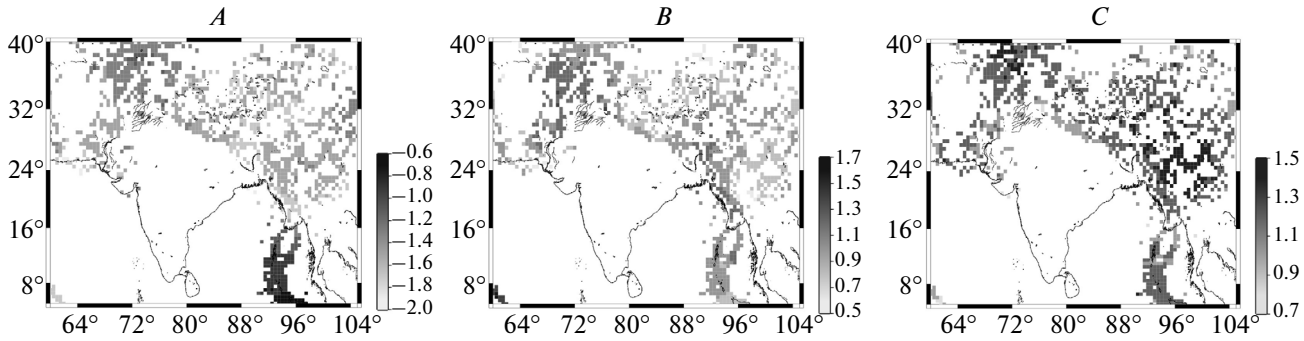

Fig. 4. Spatial distribution of the USLE coefficients, based on the USGS/NEIC Global Hypocenters Database System for the period of 1965 to 2011.

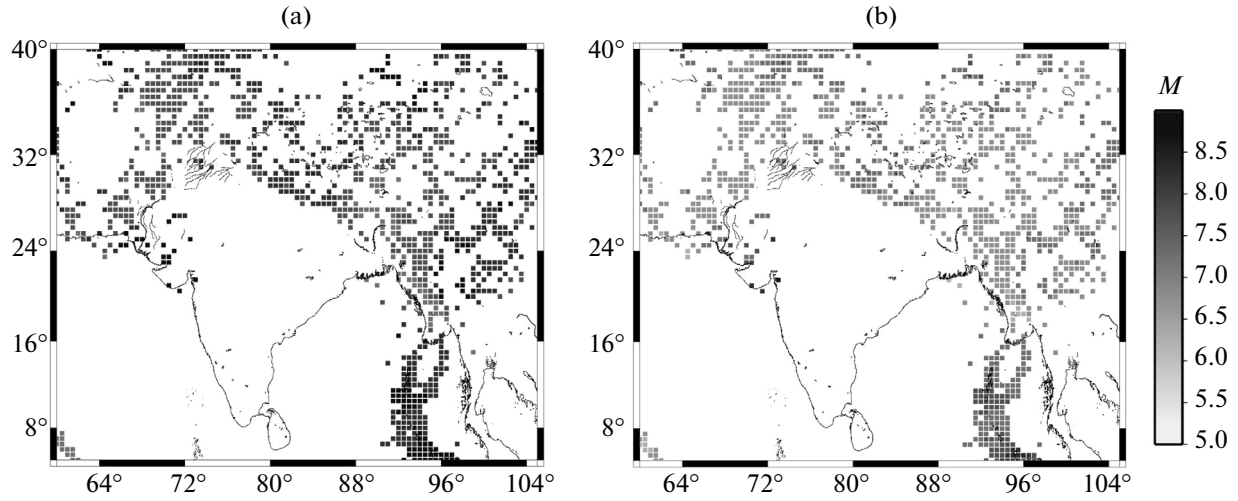

Fig. 5. The expected maximal magnitude M for a period of 50 years with the probability of its exceedance of (a) 1% and (b) 10% calculated from the USLE coefficients in Fig. 4.

with a magnitude starting from 6.0, instead of moderate earthquakes starting from magnitude 5.0 as is done in formula (1) to satisfy the completeness of the global database. The error in the determination of the numerical value of A, B, and C is at most 0.07, which confirms the declared accuracy of the mapped values.

The highest values of coefficient A in Fig. 4a are clustered in the areas of the Andaman Islands, NW Himalayas, and Pamir–Hindu Kush. Figure 4b shows that coefficient B characterizing the balance between the magnitude ranges mainly falls in the interval between 0.7 and 0.9, with the highest values clustering in the NW Himalayas, Hindu Kush, and Indo–Burnese arc. The estimate of the fractal dimension of the epicenter locus, coefficient C, has a bimodal density distribution within 0.8 to 1.5 and peaks at 1.1 and 1.25, which can be interpreted as scaling near the linear structures of the main faults and in the zones of high fragmentation of the Earth's crust. The highest values of C are mainly localized in Myanmar and Pamir–Hindu Kush. It can be seen that the distribution of coefficient C qualitatively corresponds to the degree of crustal fragmentation: the highest C indicate the most damaged marginal areas in the wide zone of collision of the continental plates.

The obtained estimates of the USLE coefficients were used for calculating two maps of the expected maximal magnitude M for a period of 50 years at 1 and 10% probability of this magnitude being exceeded (Figs. 5a and 5b, respectively). For the purposes of comparison and as an additional check of the stability of the results, the estimates of the USLE coefficients and seismic hazard maps were also calculated for a finer spatial resolution (0.125° × 0.125°) and larger number of hierarchical levels ($NH = 5$), using the data on earthquakes with magnitudes 4.0 and higher for the period of 1980 to 2011. In particular, reliable (determined with a standard error of at most 0.05) estimates of the USLE coefficients were obtained for 1574 of 1640 cells with a size of 0.25° × 0.25°. These estimates overall qualitatively agree with the maps shown in Fig. 5.

The distributions in Figs. 5a and 5b have naturally similar elements and clear distinctions. In particular,

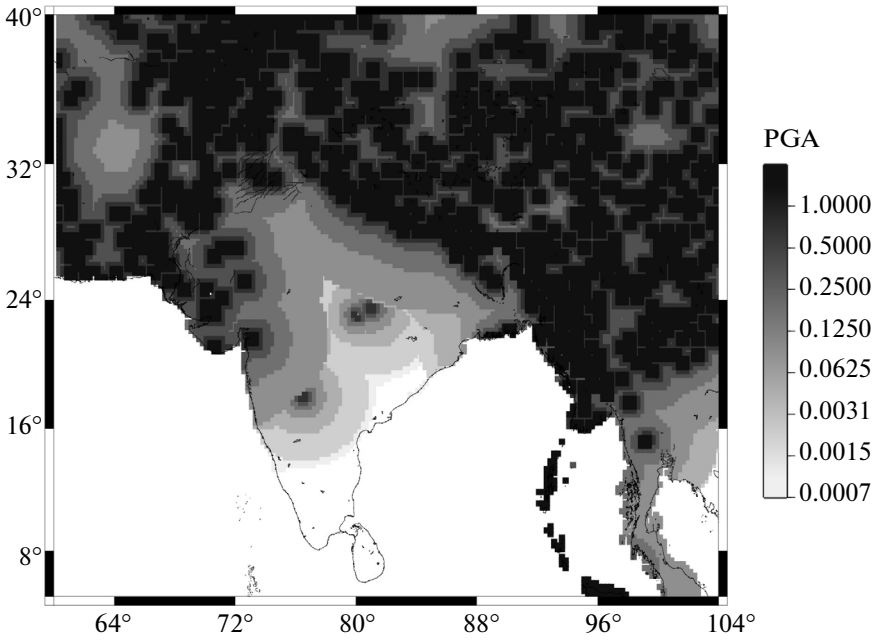

Fig. 6. Seismic hazard map.

the correlation coefficient between these two maps is 85%. The median value of the expected maximal magnitude is 8 for the map in Fig. 5a and 6.5 for the magnitudes in Fig. 5b. The maps in Fig. 5 fully agree with the results of pattern recognition of the areas that are prone to earthquakes with magnitudes 6.5, 7.0, and 8.2, based on the analysis of the geomorphologic and geodetic parameters (Bhatia et al., 1992; Kossobokov, 1984). We note that the results of recognition have been in many cases confirmed by the earthquakes that occurred after their publication (Gorshkov et al., 2003; Gorshkov, Parvez, and Novikova, 2012).

Naturally, due to the spatial and temporal incompleteness of the earthquake catalog, reliable estimates of USLE coefficients (and, correspondingly, the reliable estimates of the expected maximal magnitude M) can only be obtained for the part of the cells with the observed seismicity. Considering this, for a more complete seismic hazard assessment, in the final map, the expected maximal magnitudes M estimated from the USLE coefficients were complemented by the values of maximal observed magnitudes from the NEIC catalog for the period 1900–2010 in the cells where the USLE coefficients were absent. The final map of maximal magnitude M expanded in such a way was then used for estimating the expected ground shaking on bedrock in terms of the peak ground acceleration (PGA) by the computation methods suggested in (Parvez et al., 2001). These calculation methods, generally deterministic, are based on the empirical data on the strong ground motion in the territory of the Himalayas and the relationship between the maximal PGA and distance to an earthquake's epicenter. The map of deterministic seismic hazard assessment (Fig. 6) was obtained by calculating the source–receiver function, with the receivers located at the nodes of the $0.25° \times 0.25°$ grid and the sources at the centers of the cells with maximal expected magnitude M. For each source, in accordance with the attenuation function (Parvez et al., 2001), the PGA values were calculated in the receiver points at the distances of up to 500 km, and then the maximum of these values in the receivers were mapped. In the resulting seismic hazard map, the zones of maximal PGA (1 g and higher) clearly delineate the plate collision boundary along the Himalayas and adjacent areas, including a part of Gujarat state in the west, and the Indo–Burnese and Andaman–Nicobar arcs. Within the piedmont of the Himalayas and Indo-Gangetic Plain, the PGA values range from 0.06 to 0.2 g.

Seismic Risk Assessment

Mathematically, any type of risk is a result of the convolution of the hazard with object at risk and with the vulnerability of this object:

$$\mathrm{R}(\mathbf{g}) = \mathrm{H}(\mathbf{g}) \otimes \mathrm{O}(\mathbf{g}) \otimes \mathrm{V}(\mathrm{O}(\mathbf{g})),$$

where $\mathrm{H}(\mathbf{g})$ is the natural hazard located at $\mathbf{g}$; $\mathrm{O}(\mathbf{g})$ characterizes the objects at risk at the location $\mathbf{g}$; and $\mathrm{V}(\mathrm{O}(\mathbf{g}))$ describes the vulnerability of the risk-prone objects at the location $\mathbf{g}$. Here, $\mathbf{g}$ may either be a point, a line, or a zone on the Earth's surface or beneath it, and the distribution of hazard, as well as the distribution and vulnerability of the objects at risk can depend on time. Besides, convolution $\otimes$ can require a significantly more complex operation than commonly used multiplication of the risk components.

Thus, there are different risk assessments even for the same objects at risk that are prone to the same hazard. In particular, this can be related with the different convolution laws or depend on different types of objects' vulnerability specific to the location. Both these conceptual questions should be addressed by the interdisciplinary problem-oriented studies by the experts dealing with the particular hazards, objects, and vulnerabilities. In order to illustrate the general concept, we considered four simplified convolutions of the estimate of seismic hazard $\mathbf{H(g)}$ shown in Fig. 6, with the population as the object at risk $\mathbf{O(g)}$, which is shown in Fig. 3 in the map of the population density per km^2.

Each of the four seismic hazard assessments considers the GPWv3 model of the demographic data for 2010 as the object at risk and uses multiplication as the convolution. The first seismic risk assessment in the location $\mathbf{g}$ ($0.25° \times 0.25°$ grid cell) is based on a constant that is equal to the vulnerability of every individual, $R_i(\mathbf{g}) = H(\mathbf{g}) \cdot \int_{\mathbf{g}} P$, where $\int_{\mathbf{g}} P$ is the integral of the population density in the cell $\mathbf{g}$ (i.e., the number of individuals located within the area of the cell $\mathbf{g}$). The second seismic risk assessment distinguishes the personal vulnerability, which linearly increases with the population density at a given locality, $R_{ii}(\mathbf{g}) = H(\mathbf{g}) \cdot \int_{\mathbf{g}} P \cdot P$. This assessment and the two remaining nonlinear risk assessments ($R_{iii}(\mathbf{g}) = H(\mathbf{g}) \cdot \int_{\mathbf{g}} P \cdot P^2$ and $R_{iv}(\mathbf{g}) = H(\mathbf{g}) \cdot \int_{\mathbf{g}} P \cdot P^3$) appear to be quite natural due to the specifics of the man-made environment, which is determined by the amount and density of the population in heavily populated areas (for example, the number of floors or the categories of typical buildings). These seismic risk assessments resulted in the four maps presented in Fig. 7. For illustration, each of the four arbitrary units of risk covers the seven highest decimal orders of magnitude of the obtained values so that the black cells are by a factor of 1 000 000 more risky than the lightest gray cells. The collapse of the high-risk areas to the highest populated zones is quite a natural and clear illustration of how the nonlinearity in the initial conditions changes the notion of the seismic risk. It can be seen that the largest cities and their agglomerations fall in the upper part of the distribution for each risk considered here, which is quite expectable.

In order to avoid misleading counter-productive interpretations, risk assessments for the discussed territory are only provided for methodological research purposes. Our estimates do not use more sophisticated complex procedures, which can turn out to be more adequate convolutions of the hazards, objects at risk, and vulnerability. The risk estimates are only used here to illustrate the general problem-oriented approach. The practical and therefore realistic seismic risk assessments should be developed by the experts in seismic hazard distribution and objects at risk of different vulnerability (i.e., specialists in seismic zoning, earthquake engineering, social sciences, and economic sciences).

DISCUSSION AND CONCLUSIONS

The time and place of a future seismic event is unpredictable up to the exact date and place of the source rupture. Although the possibility of intermediate-term earthquake forecasting with a medium spatial resolution has been proven by the results of the long-lasting global experiment, there is no link yet for implementing the measures of preparedness for earthquakes in response to the diagnosis of the periods of high hazard (Kossobokov, 2012; Davis et al., 2012). The damage from earthquakes can be efficiently reduced by using the forecasts of the strongest earthquakes with the known level of reliability and accuracy. Unfortunately, the practice of using the reliable intermediate-term earthquake forecasts for making decisions on particular measures to increase seismic safety is currently very limited due to the ethical restrictions of privacy in the announcement of forecasts.

On the other hand, earthquake-prone areas all over the world are well known from seismic observations and geological studies. Strong catastrophic earthquakes are lowprobability events; however, in the earthquake-prone areas they occur with certainty (i.e., with 100% probability). The long return period and/or low probability of the earthquake, being suggested as the basis of seismic hazard assessment, leads to false illusion of safety and neglecting these rare occasions. With this approach, the strong earthquakes will repeatedly occur as unpredictable catastrophic surprises. Unfortunately, the systematic quantitative examination of the map obtained in the Global Seismic Hazard Assessment Program (GSHAP, see (Giardini, 1999)) has established the unacceptable inadequacy of this probabilistic forecasting tool (Kossobokov and Nekrasova, 2012): all the sixty earthquakes with magnitudes starting from 7.5 that occurred in 2000–2009, after the publication of the GSHAP maps, turned out to be surprises; moreover, half of them were big surprises that caused a shaking intensity significantly exceeding the values suggested by the map. The same applies for the twelve deadliest earthquakes that occurred in 2000–2011 and caused the highest death tolls (over 700 000 people in total). These and the other self-evident shortcomings and failures of the widespread probabilistic approach to seismic hazard assessment indicate that the GSHAP map and the underlying methods are misleading. From the common-sense viewpoint, using these maps for any responsible seismic hazard assessment is unacceptable as they do not prepare the public for potential disasters. Other modern methods of modeling realistic

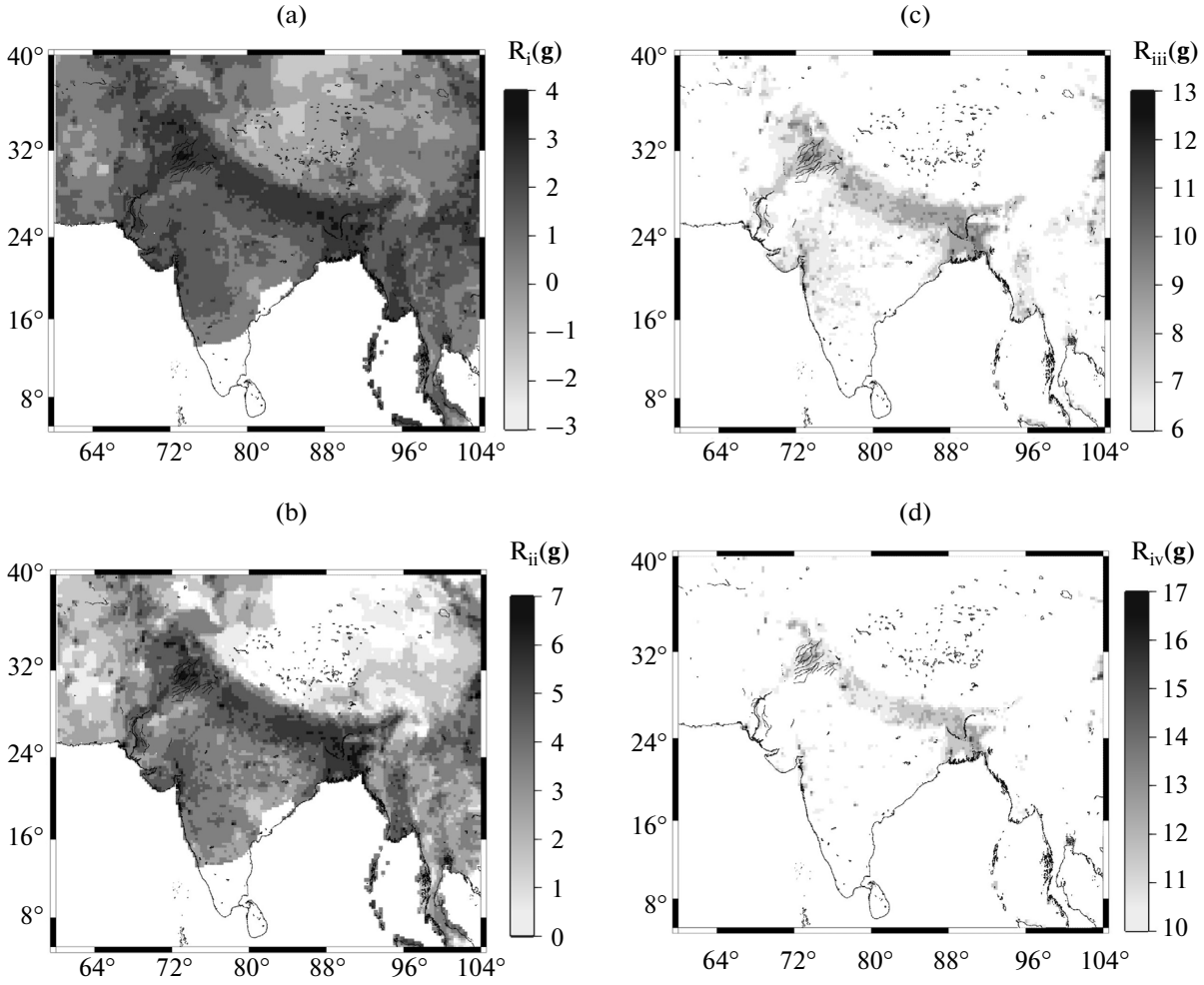

Fig. 7. The maps of simplified convolutions of seismic hazard $H(\mathbf{g})$ and population density P: (a) $R_i(\mathbf{g}) = H(\mathbf{g}) \cdot \int_{\mathbf{g}} P$, (b) $R_{ii}(\mathbf{g}) = H(\mathbf{g}) \cdot \int_{\mathbf{g}} P \cdot P$; (c) $R_{iii}(\mathbf{g}) = H(\mathbf{g}) \cdot \int_{\mathbf{g}} P \cdot P^2$; (d) $R_{iv}(\mathbf{g}) = H(\mathbf{g}) \cdot \int_{\mathbf{g}} P \cdot P^3$.

earthquake scenarios allow the seismic hazard to be assessed certainly better (Panza et al., 2011).

At present, the damage and casualties from disasters keep steadily growing due to the absence of the necessary knowledge and incomplete understanding by the scientific community, decision-making authorities, and the public of the three major risk components: hazard, object at risk, and vulnerability. Modern science (in particular, geophysics and seismology) is largely responsible for failures in managing the changes of risk components caused by the growth and density of the population, etc. Due to their special education, knowledge, and skills, scientists are responsible for the safety of society, which generally lacks this special knowledge. The errors in seismic hazard assessment are nonlinearly transformed into inadmissible errors of the expected human deaths and economic losses (Wyss et al., 2012).

The maximal magnitude of an expected earthquake for seismically hazardous areas can be realistically estimated with high reliability. The preparedness to the maximal possible events helps reducing the scale or even avoiding the probable consequences. Human deaths do not directly follow from seismic events themselves but are rather associated with the earthquake-induced phenomena (tsunamis, landslides, collapses of buildings, bridges, and other constructions). The deterministic scenarios of the consequences of a catastrophic earthquake serve as the basis for decision-making in organizing the safety measures starting from land-use planning and adjusting the building codes and regulations for emergency management. There are many earthquake-related risks, and they must not be ignored in a realistic and responsible seismic hazard assessment and in the informed choice of the optimal measures to prevent these disasters.

Our study is an attempt to contribute to the substantiation of the urgent revision of the seismic hazard maps starting from their first principles including the choice of basic methodology and possibilities to make

use of the estimates in the calculations of seismic risks.

ACKNOWLEDGMENTS

The work was supported by the Russian Foundation for Basic Research (projects 14-05-92691_IND_a, 13-05-91167_GFEN, 11-05-92691_IND_a), and by the Department of Science and Technology of the Government of India (grant DTS INT/RFBR/P-176).

REFERENCES

Auden, J.B., Earthquakes in relation to the Damodar Valley Project, *Proc. Symp. Earthquake Eng.*, Roorkee: 1st Univ. Roorkee, 1959.

Bak, P., Christensen, K., Danon, L., and Scanlon, T., Unified scaling law for earthquakes, *Phys. Rev. Lett.*, 2002, vol. 88, pp. 178501–178504.

Bhatia, S.C., Chetty, T.R.K., Filimonov, M., Gorshkov, A., Rantsman, E., and Rao, M.N., Identification of potential areas for the occurrence of strong earthquakes in Himalayan arc region, *Proc. Indian Acad. Sci., Earth Planet. Sci.*, 1992, vol. 101, no. 4, pp. 369–385.

Bhatia, S.C., Kumar, R., and Gupta, H.K., A probabilistic seismic hazard map of India and adjoining regions, *Ann. Geofis.*, 1999, vol. 42, pp. 1153–1164.

Christensen, K., Danon, L., Scanlon, T., and Bak, P., Unified scaling law for earthquakes, *Proc. Natl. Acad. Sci.*, 2002, vol. 99 (Suppl. 1), pp. 2509–2513.

Davis, C., Keilis-Borok, V., Kossobokov, V., and Soloviev, A., Advance prediction of the March 11, 2011 Great East Japan earthquake: a missed opportunity for disaster preparedness, *Int. J. Disaster Risk Reduct.*, 2012, no. 1, pp. 17–32. doi: 10.1016/j.ijdrr.2012.03.001

Gaur, V.K. and Chouhan, R.K.S., Quantitative measures of seismicity applied to Indian regions, *Bull. Indian Soc. Earthquake Technol.*, 1968, no. 5, pp. 63–78.

Giardini, D., Grunthal, G., Shedlock, K.M., and Zhang, P., The GSHAP global seismic hazard map, *Ann. Geofis.*, 1999, vol. 42, no. 6, pp. 1225–1230.

Gorshkov, A., Kossobokov, V., and Soloviev, A., Recognition of earthquake-prone areas, in *Nonlinear Dynamics of the Lithosphere and Earthquake Prediction*, Keilis-Borok, V.I. and Soloviev, A.A., Eds., Heidelberg: Springer, 2003, pp. 239–310.

Gorshkov, A., Parvez, I.A., and Novikova, O., Recognition of earthquake-prone areas in the Himalaya: validity of the results, *Int. J. Geophys.*, 2012. doi 10.1155/2012/419143

Gridded Population of the Worlds, Version 3 (GPWv3), 2005. Palisades: SEDAC, Columbia Univ. http://sedac.ciesin.columbia.edu/gpw. [2012.05.29].

Kaila, K.L. and Rao, M., Seismic zoning maps of Indian subcontinent, *Geophys. Res. Bull.*, 1979, vol. 17, pp. 293–301.

Keilis-Borok, V.I., Kossobokov, V.G., and Mazhkenov, S.A., On the similarity in spatial distribution of seismicity, in *Vychislitel'naya seismologiya, vyp. 22: Teoriya i algoritmy interpretatsii geofizicheskikh dannykh* (Computational Seismology, vol. 22: Theory and Algorithms of Interpretation of Geophysical Data), 1989, pp. 28–40.

Keilis-Borok, V.I., The lithosphere of the Earth as a nonlinear system with implications for earthquake prediction, *Rev. Geophys.*, 1990, vol. 28, no. 1, pp. 19–34.

Khattri, K.N., Rogers, A.M., Perkins, D.M., and Algermissen, S.T., A seismic hazard map of India and adjacent areas, *Tectonophysics*, 1984, vol. 108, pp. 93–134.

Kossobokov, V.G., General features of the strongest (with $M \geq 8.2$) earthquake-prone areas in the non-Alpine zone of the Transasian seismic belt, *Comput. Seismol.*, 1984, vol. 17: *Logical and Computational Methods in Seismology*, Keilis-Borok, V.I. and Levshin, A.L., Eds., Moscow: Nauka, pp. 69–72.

Kossobokov, V.G. and Mazhkenov, S.A., Spatial characteristics of similarity for earthquake sequences: fractality of seismicity, in *Lecture Notes of the Workshop on Global Geophysical Informatics with Applications to Research in Earthquake Prediction and Reduction of Seismic Risk*, Trieste: ICTP, 1988.

Kossobokov, V.G. and Mazhkenov, S.A., On similarity in the spatial distribution of seismicity, *Comput. Seismol. Geodyn.*, 1994, no. 1, pp. 6–15.

Kossobokov, V.G. and Nekrasova, A.K., Generalized Gutenberg–Richter law, *Geophys. Res. Abstr.*, 2003, EAE03-A-06597.

Kossobokov, V.G. and Nekrasova, A.K., General similarity law for earthquakes: global map of the parameters, in *Vychislitel'naya seismologiya, vyp. 35: Analiz geodinamicheskikh i seismicheskikh protsessov* (Computational Seismology, col. 35: Analysis of Geodynamical and Seismic Processes), Moscow: GEOS, 2004, pp. 160–175.

Kossobokov, V.G., Earthquake prediction: 20 years of global experiment *Nat. Hazards*, 2012. doi 10.1007/s11069-012-0198-1

Kossobokov, V.G. and Nekrasova, A.K., Global Seismic Hazard Assessment Program maps are erroneous, *Seism. Instrum.*, 2012, vol. 48, no. 2, pp. 162–170. doi: 10.3103/S0747923912020065

Lyubushin, A. and Parvez, I.A., Map of seismic hazard of India using Bayesian approach, *Nat. Hazards*, 2010, vol. 55, pp. 543–556.

Mandelbrot, B.B., *The Fractal Geometry of Nature*, New York: Freeman, 1982.

Molchan, G., Kronrod, T., Panza, G.F., Multi-scale seismicity model for seismic risk, *Bull. Sesimol. Soc. Am.*, 1997, vol. 87, pp. 1220–1229.

Nekrasova, A. and Kossobokov, V., Generalizing the Gutenberg-Richter scaling law, *Trans., Am. Geophys. Union*, 2002, vol. 83 (47), NG62B-0958.

Nekrasova, A.K. and Kossobokov, V.G., Temporal variations in the parameters of the unified scaling law for earthquakes in the eastern part of Honshu Island (Japan), *Dokl. Earth Sci.*, 2005, vol. 405, no. 9, pp. 1352–1355.

Nekrasova, A.K. and Kossobokov, V.G., General law of similarity for earthquakes: evidence from the Baikal Region, *Dokl. Earth Sci.*, 2006, vol. 407A, no. 3, pp. 484–485.

Nekrasova, A.K., General similarity law for earthquakes: an application to seismoactive regions of the world, *Cand. (Phys.-Math.) Sci. Dissertation*, Moscow: Inst. Earthquake

Prediction Theory and Math. Geophys., Russian Academy of Sciences, 2008.

Nekrasova, A., Kossobokov, V., Peresan, A., Aoudia, A., and Panza, G.F., A multiscale application of the unified scaling law for earthquakes in the Central Mediterranean Area and Alpine Region, *Pure Appl. Geophys.*, 2011, vol. 168, pp. 297–327.

Okubo, P.G. and Aki, K., Fractal geometry in the San Andreas Fault system, *J. Geophys. Res.*, 1987, vol. 92 (B1), pp. 345–356.

Panza, G., Irikura, K., Kouteva-Guentcheva, M., Peresan, A., Wang, Z., and Saragoni, R., Eds., Advanced Seismic Hazard Assessment, *Pure Appl. Geophys.*, 2011, vol. 168, nos. 1–4.

Parvez, I.A. and Ram, A., Probabilistic assessment of earthquake hazards in the north-east Indian peninsula and Hindukush region, *Pure Appl. Geophys.*, 1997, vol. 149, pp. 731–746.

Parvez, I.A. and Ram, A., Probabilistic assessment of earthquake hazards in the Indian subcontinent, *Pure Appl. Geophys.*, 1999, vol. 154, pp. 23–40.

Parvez, I.A., Gusev, A.A., Panza, G.F., and Petukhin, A.G., Preliminary determination of the interdependence among strong motion amplitude, earthquake magnitude and hypocentral distance for the Himalayan region, *Geophys. J. Int.*, 2001, vol. 144, pp. 577–596.

Parvez, I.A., Vaccari, F., and Panza, G.F., A deterministic seismic hazard map of India and adjacent areas, *Geophys. J. Int.*, 2003, vol. 155, pp. 489–508.

Parvez, I.A., On the Bayesian analysis of the earthquake hazard in the North-East Indian peninsula, *Nat. Hazards*, 2007, vol. 40, pp. 397–412.

Sadovskii, M.A., Bolkhovitinov, L.G., and Pisarenko, V.F., On the discreteness property of rocks, *Izv. Akad. Nauk SSSR, Fiz. Zemli*, 1982, no. 12, pp. 3–18.

Sadovskii, M.A., Golubeva, T.V., Pisarenko, V.F., and Shnirman, M.G., Characteristic sizes of a rock and hierarchic properties of seismicity, *Izv. Akad. Nauk SSSR, Fiz. Zemli*, 1984, no. 20, pp. 87–96.

Turcotte, D.L., *Fractals and Chaos in Geology and Geophysics*, 2nd ed., Cambridge: Cambridge Univ. Press, 1997.

Turcotte, D.L., Seismicity and self-organized criticality, *Phys. Earth Planet. Inter.*, 1999, vol. 111, pp. 275–294.

Wyss, M., Nekrasova, A., and Kossobokov, V., Errors in expected human losses due to incorrect seismic hazard estimates, *Nat. Hazards*, 2012, vol. 62, no. 3, pp. 927–935.

Translated by N. Astafiev